


Cite this: *RSC Adv.*, 2023, 13, 7828

1,10-Phenanthroline-based periodic mesoporous organosilica: from its synthesis to its application in the cobalt-catalyzed alkyne hydrosilylation†

Xiao-Tao Lin,^{ab} Yusuke Ishizaka,^{ID} ^a Yoshifumi Maegawa,^c Katsuhiko Takeuchi,^{ID} ^a Shinji Inagaki,^{ID} ^{*ac} Kazuhiro Matsumoto^{ID} ^{*a} and Jun-Chul Choi^{ID} ^{*ab}

1,10-Phenanthroline (Phen) is a typical ligand for metal complexation and various metal/Phen complexes have been applied as a catalyst in several organic transformations. This study reports the synthesis of a Phen-based periodic mesoporous organosilica (Phen-PMO) with the Phen moieties being directly incorporated into the organosilica framework. The Phen-PMO precursor, 3,8-bis[(triisopropoxysilyl)methyl]-1,10-phenanthroline (**1a**), was prepared *via* the Kumada–Tamao–Corriu cross-coupling of 3,8-dibromo-1,10-phenanthroline and [(triisopropoxysilyl)methyl]magnesium chloride. The co-condensation of **1a** and 1,2-bis(triethoxysilyl)ethane in the presence of P123 as the template surfactant afforded Phen-PMO **3** with an ordered 2-D hexagonal mesoporous structure as confirmed by nitrogen adsorption/desorption measurements, X-ray diffraction, and transition electron microscopy. Co(OAc)₂ was immobilized on Phen-PMO **3**, and the obtained complex showed good catalytic activity for the hydrosilylation reaction of phenylacetylene with phenylsilane.

Received 28th December 2022

Accepted 1st March 2023

DOI: 10.1039/d2ra08272a

rsc.li/rsc-advances

Introduction

In 1999, periodic mesoporous organosilica (PMO) materials were developed independently by three groups, Inagaki, Ozin, and Stein.^{1–3} Since then, these materials have been attracting attention as organic/inorganic hybrid materials owing to their ordered mesoporous structures.⁴ In particular, PMOs are promising candidates in catalysis, where they are used as solid ligands to immobilize active metal complexes in the mesopores.⁵ While the direct incorporation of pre-formed metal complexes into organosilica frameworks during the synthesis of PMOs has been already reported,⁶ PMOs can act as versatile solid ligands by (a) the direct incorporation of a coordination site into the organosilica framework followed by complexation,^{7,8} or (b) the post-functionalization of PMOs by grafting a metal complex/a coordination site *via* the surface silanol groups or functional groups integrated into the organosilica framework.⁹

In the direct incorporation approach, 2,2'-bipyridine-based periodic mesoporous organosilica (BPy-PMO), prepared from

a 5,5'-bis(triisopropoxysilyl)-2,2'-bipyridine precursor, has been the most widely developed solid ligand for an array of metal complexes.^{7,10} The immobilized complexes obtained by this approach have been employed as catalysts for various organic transformations and photocatalytic reactions. Furthermore, the synthesis of BPy-PMO analogs that fine-tune the catalytic activity and/or impart new reactivity have been reported,¹¹ which can further enhance the potential of PMOs in catalysis.

1,10-Phenanthroline (Phen) has a coordination geometry similar to 2,2'-bipyridine because both have two sp² nitrogen atoms and can form five-membered chelates upon their coordination with a metal center.¹² The C2–C2' bond of 2,2'-bipyridine can rotate freely, whereas Phen possesses a more rigid planar geometry because of the additional –HC=CH– bridge. Therefore, the two sp² nitrogen atoms of Phen are juxtaposed to readily form a chelate. Furthermore, the additional bridge extends its π -conjugated system. Consequently, Phen and 2,2'-bipyridine sometimes exhibit different catalytic activities when applied as ligands for metal complexes.¹³

Several Phen-PMOs, in which the Phen moieties have been directly incorporated into the organosilica framework, have been previously reported (Fig. 1a).¹⁴ In these precursors, trialkoxysilyl groups are connected to the Phen moiety at the 5,6 or 5 position(s) through a conformationally flexible propylene linker with a urea or urethane function. This study reports the synthesis and characterization of a novel class of Phen-PMOs, in which the trialkoxysilyl group was linked to Phen at the 3,8 positions *via* a less flexible methylene linker (Fig. 1b). The immobilization of Co(OAc)₂ on the as-synthesized Phen-PMO

^aNational Institute of Advanced Industrial Science and Technology (AIST), Tsukuba Central 5, 1-1-1 Higashi, Tsukuba, Ibaraki 305-8565, Japan. E-mail: kazuhiro.matsumoto@aist.go.jp; junchul.choi@aist.go.jp

^bGraduate School of Pure and Applied Sciences, University of Tsukuba, 1-1-1 Tennodai, Tsukuba, Ibaraki 305-8573, Japan

^cToyota Central R&D Labs., Inc., Nagakute, Aichi 480-1192, Japan

† Electronic supplementary information (ESI) available. See DOI: <https://doi.org/10.1039/d2ra08272a>



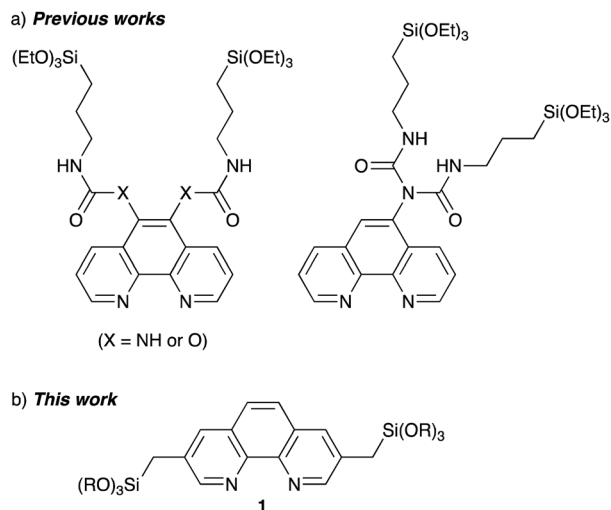


Fig. 1 Phen-PMO precursors in (a) previous works and (b) this work.

and its preliminary application as an immobilized catalyst for alkyne hydrosilylation are also investigated.

Results and discussion

Synthesis of the Phen-PMO precursor

Although Phen derivative **2** bearing trialkoxysilyl groups directly at the 3,8 positions is a possible precursor for Phen-PMOs, precursor **2** might decompose by proto-desilylation during the preparation of PMOs, especially under acidic conditions (Fig. 2).¹⁵ The extended π -conjugated system of 1,10-phenanthroline would promote protonation on the *ipso*-carbon atom by stabilizing the corresponding σ -complex, thus resulting in proto-desilylation. Consequently, Phen derivative **1** incorporating trialkoxysilylmethyl groups at the 3,8 positions was synthesized as a Phen-PMO precursor. Since the trialkoxysilyl group is attached to the Phen moiety through an sp^3 carbon atom, the proto-desilylation reaction was not expected to proceed.

A straightforward route for the synthesis of Phen-PMO precursor **1** is *via* the cross-coupling of 3,8-halo-1,10-phenanthroline and a [(trialkoxysilyl)methyl]metal reagent. However, the Phen moiety exhibits a potent coordination ability with the metal center, so its coordination to transition metal

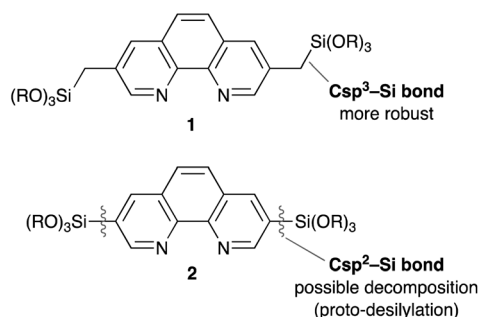
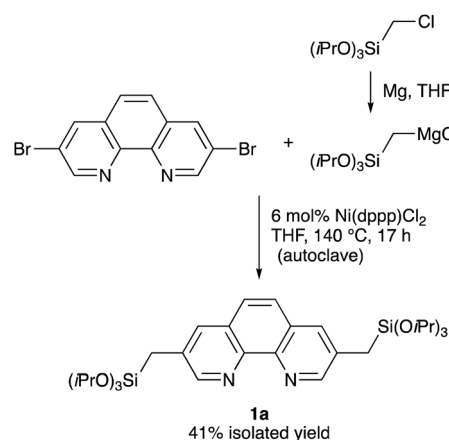


Fig. 2 Comparison of Phen-PMO precursor candidates **1** and **2**.

catalysts for the desired cross-coupling should be avoided. Therefore, the Kumada-Tamao-Corriu cross-coupling, a robust C-C bond formation reaction, was employed for the synthesis of Phen-PMO precursor **1** (Scheme 1). The Kumada-Tamao-Corriu cross-coupling of the commercially available 3,8-dibromo-1,10-phenanthroline and [(triisopropoxysilyl)methyl]magnesium chloride,¹⁶ prepared from (chloromethyl)triisopropoxysilane and magnesium powder in THF, was carried out in the presence of Ni(dppp)Cl₂ (6 mol%) at 140 °C in an autoclave with a PTFE inner vessel. Consequently, 3,8-bis[(triisopropoxysilyl)methyl]-1,10-phenanthroline (**1a**) was isolated in a moderate but acceptable yield (41%) (Table 1, entry 1). High temperatures were essential for the desired cross-coupling reaction to proceed. Under reflux conditions (THF: bp 66 °C) and in a standard glassware, only a trace amount of **1a** was detected (entry 2). Performing the reaction in an autoclave at 90 °C afforded **1a** in a slightly lower yield (entry 3). The yield decreased in the presence of dppe ligand having a narrower bite angle and dppf with a wider bite angle than dppp (entries 4 and 5).

Synthesis and characterization of Phen-PMO

The synthesis of Phen-PMO using **1a** as the sole precursor did not afford any mesoporous materials. Consequently, the co-condensation of **1a** and 1,2-bis(triethoxysilyl)ethane (BTEE) was investigated in the presence of three template surfactants: C₂₂TMAcI, polyoxyethylene(10) stearyl ether (Brij76), and poly(ethylene glycol)-*block*-poly(propylene glycol)-*block*-poly(ethylene glycol) (P123). The co-condensation in the presence of C₂₂TMAcI as an ionic template surfactant under basic conditions resulted in the partial cleavage of the Si-C bonds of the precursor, as indicated by the detection of peaks corresponding to the Q units around -100 ppm in the ²⁹Si dipolar decoupling/magic-angle spinning (DD/MAS) NMR spectroscopy (Fig. S1†). In the presence of Brij76 as a nonionic surfactant template under acidic conditions, the Si-C bond cleavage was sufficiently suppressed (Fig. S2†), and the formation of a mesoporous structure was confirmed by the nitrogen (N₂) adsorption/desorption analysis which exhibited a typical type IV isotherm (Fig. S3†). However, transmission electron microscopy (TEM)



Scheme 1 Synthesis of Phen-PMO precursor **1a**.



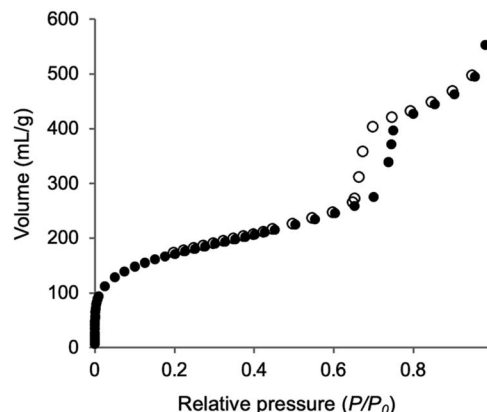
Table 1 Optimization of nickel/diphosphine catalysts and reaction temperature

Entry	Cat.	<i>T</i> (°C)	Yield ^a (%)
1	Ni(dppp)Cl ₂	140	56 (41) ^b
2 ^c	Ni(dppp)Cl ₂	66 (reflux)	Trace
3	Ni(dppp)Cl ₂	90	53
4	Ni(dppe)Cl ₂	140	46
5	Ni(dppf)Cl ₂	140	46

^a Determined by ¹H NMR analysis using mesitylene as internal standard. ^b Isolated yield. ^c Reaction was carried out in a glassware.

images revealed that the obtained Phen-PMO had a disordered structure (Fig. S4†). An ordered 2-D hexagonal mesoporous material, Phen-PMO 3, was obtained when the co-condensation was performed in the presence of P123 and KCl under acidic conditions (Scheme 2).

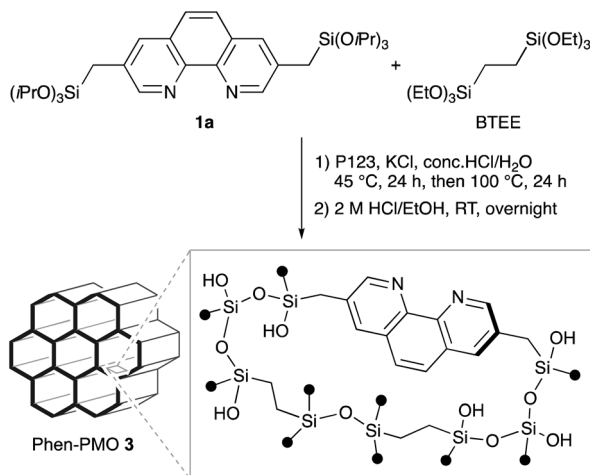
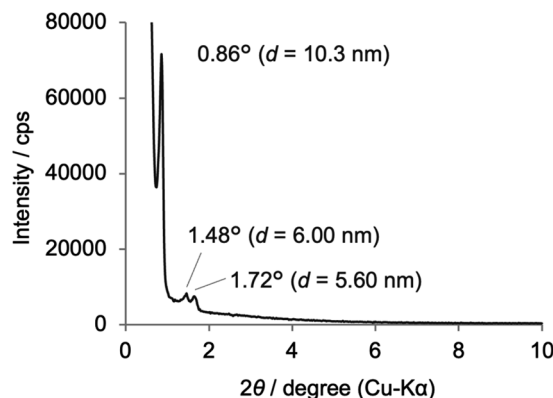
The incorporation of the Phen unit of **1a** and the ethylene unit of BTEE into Phen-PMO 3 was confirmed by the ¹³C cross-polarization (CP)/MAS NMR spectroscopy (Fig. S5†). Furthermore, the ²⁹Si CP/MAS NMR spectrum of **3** showed peaks corresponding to the *T*² and *T*³ units in the −50 to −70 ppm range (Fig. S6†). Moreover, significant peaks corresponding to the *Q* units around −100 ppm were not observed, thus indicating that the Si–C bonds of the precursors were maintained in Phen-PMO 3. The amount of Phen units introduced into Phen-PMO 3 was 0.75 mmol g^{−1} as calculated from the nitrogen content (2.1%) determined by elemental analysis. The N₂ adsorption/desorption analysis showed a type IV isotherm with hysteresis in the relative pressure (*P*/*P*₀) range from 0.65 to 0.75, which indicated the formation of a mesoporous structure (Fig. 3). The Brunauer–Emmett–Teller surface area (*S*_{BET}) and pore diameter (*d*_{B_{JH}}) were 607 m² g^{−1} and 8.2 nm, respectively. The X-ray diffraction (XRD) analysis of Phen-PMO 3 showed a sharp peak at 2θ = 0.86° (*d* = 10.3 nm) with two diffraction peaks at 2θ = 1.48° (*d* = 6.00 nm) and 1.72° (*d* = 5.60 nm), corresponding to the 2-D hexagonal lattice (*a*₀ = 12.0 nm) (Fig. 4). The absence of a peak at the medium scattering angles indicated that the

**Fig. 3** N₂ adsorption/desorption isotherm of Phen-PMO 3 (closed symbols: adsorption; open symbols: desorption).

organosilica wall constructed by the co-condensation of Phen-PMO precursor **1a** and BTEE was amorphous, unlike the crystal-like BPy-PMO and PEPy-PMO in which the organic units are regularly arranged in the pore wall (PEPy = pyridinylethynylpyridine).^{7,17} The thickness of the pore wall was 3.8 nm calculated by subtracting the pore diameter (*d*_{B_{JH}}) from the lattice constant (*a*₀). The TEM images of Phen-PMO 3 confirmed the formation of a 2-D hexagonal mesoscopically ordered structure (Fig. 5a) and uniform 1-D channels much longer than 100 nm (Fig. 5b). The channel size was in the 8–10 nm range, which was consistent with that obtained by N₂ adsorption isotherm (8.2 nm).

Immobilization of Co(OAc)₂ on Phen-PMO and its application in alkyne hydrosilylation

In order to examine the potential of Phen-PMO 3 as a solid ligand to immobilize metal complexes, the immobilization of Co(OAc)₂ onto Phen-PMO 3 was investigated (Scheme 3). The immobilization was achieved by simply mixing Co(OAc)₂ and Phen-PMO 3 in EtOH at 60 °C at an initial molar ratio of 1/2 (Co/Phen units) to obtain Co(OAc)₂@Phen-PMO 4. The immobilized Co content was 0.21 mmol g^{−1} determined by inductively coupled plasma atomic emission spectroscopy (ICP-AES), thus indicating that approximately 30% of Phen units introduced

**Scheme 2** Synthesis of Phen-PMO 3.**Fig. 4** XRD pattern of Phen-PMO 3.

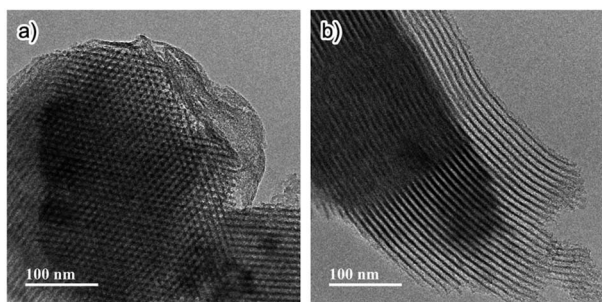
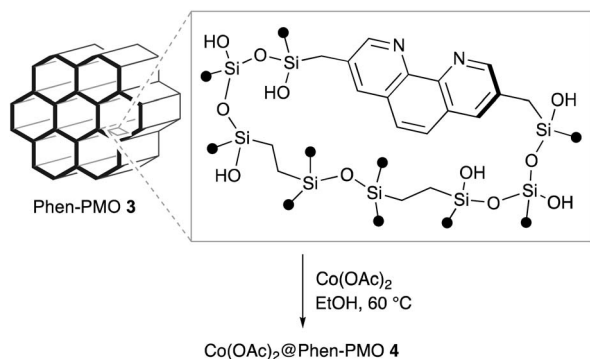


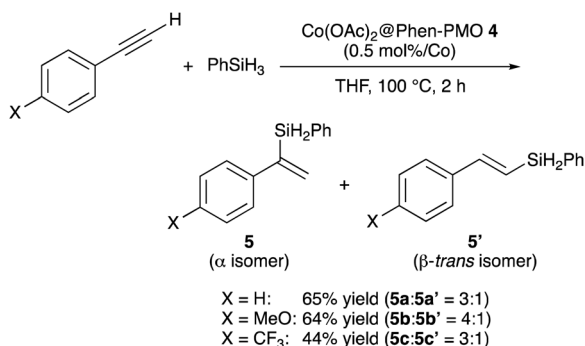
Fig. 5 TEM images (a) and (b) of Phen-PMO 3.



Scheme 3 Synthesis of $\text{Co}(\text{OAc})_2@ \text{Phen-PMO 4}$.

into Phen-PMO 3 was coordinated with Co. Due to the thickness and amorphous nature of the organosilica walls, Phen-PMO 3 could contain less accessible and even inaccessible Phen moieties.

The catalytic performance of $\text{Co}(\text{OAc})_2@ \text{Phen-PMO 4}$ was preliminary investigated in the hydrosilylation reaction of phenylacetylene with phenylsilane (Scheme 4).¹⁸ In the presence of a catalytic amount of $\text{Co}(\text{OAc})_2@ \text{Phen-PMO 4}$ (0.5 mol%/Co), phenylacetylene underwent the hydrosilylation to give the corresponding alkenylsilanes, α -isomer **5a** and β -trans-isomer **5a'**, in 65% yield and at a 3 : 1 ratio (see also Table S1†). The introduction of an electron-donating methoxy group at the *para*-position did not affect the yield but slightly improved the regioselectivity. The reaction of a phenylacetylene derivative



Scheme 4 Hydrosilylation of phenylacetylene derivatives catalyzed by $\text{Co}(\text{OAc})_2@ \text{Phen-PMO 4}$.

with an electron-withdrawing trifluoromethyl group resulted in a lower yield of 44%. The reaction did not proceed with $\text{Co}(\text{OAc})_2$ in the absence of any external ligands under the studied conditions, whereas a homogeneous counterpart, a combination of $\text{Co}(\text{OAc})_2$ and 1,10-phenanthroline, afforded the alkenylsilanes **5a** and **5a'** with a 10 : 1 ratio in 53% yield. It was thus assumed that the cobalt species which coordinated to the Phen moieties was the active catalyst. Although the detailed reaction mechanism and the structure of the active species are still unclear, the mesopore wall in which the Phen moieties are embedded would affect the regioselectivity. Since ligands can control the regioselectivity in cobalt-catalyzed hydrosilylation of terminal alkynes,^{19–21} $\text{Co}(\text{OAc})_2@ \text{Phen-PMO 4}$ which has the unique steric hindrance around the Phen moieties showed the different regioselectivity from the combination of $\text{Co}(\text{OAc})_2$ and 1,10-phenanthroline. Although we attempted catalyst recycle experiments, the $\text{Co}(\text{OAc})_2@ \text{Phen-PMO 4}$ recovered by filtration under a N_2 atmosphere after the first hydrosilylation cycle of phenylacetylene with phenylsilane showed diminished yield of 5% in the second hydrosilylation cycle.

Experimental

General information

All experiments were performed under nitrogen atmosphere using either the Schlenk technique or a glove box. All chemicals were purchased from Kanto Chemical Co., Inc., FUJIFILM Wako Chemicals, Sigma-Aldrich, or Tokyo Chemical Industry (TCI), and used as received without further purification. 3,8-Dibromo-1,10-phenanthroline was prepared according to a previously reported procedure.²² Silica gel column chromatography was performed on a Yamazen AI-580 Single Channel Automated Flash Chromatography System. ^1H , $^{13}\text{C}\{^1\text{H}\}$ and $^{29}\text{Si}\{^1\text{H}\}$ NMR spectra were recorded on a Bruker AVANCE III HD NMR spectrometer (^1H NMR at 600 MHz; $^{13}\text{C}\{^1\text{H}\}$ NMR at 151 MHz; $^{29}\text{Si}\{^1\text{H}\}$ NMR at 119 MHz). ^{13}C CP/MAS NMR and ^{29}Si CP/MAS NMR measurements were performed using a 4 mm diameter ZrO_2 rotor at a sample spinning frequency of 8 kHz using a Bruker AVANCE II NMR spectrometer (^{13}C CP/MAS NMR at 100.6 MHz; ^{29}Si CP/MAS NMR at 79.49 MHz). ICP-AES was performed on a Hitachi High-Tech PS3520VDDII in the Toray Research Center, Inc. Nitrogen adsorption/desorption isotherms were measured using a MicrotracBEL BELSORP MAX-II instrument. BET surface areas were calculated from the linear sections of the BET plots ($P/P_0 = 0.1$ – 0.2). Pore-size distributions were calculated from adsorption branch using the Barrett-Joyner-Halenda (BJH) method. XRD patterns were recorded on a Rigaku RINT-TTR diffractometer under $\text{Cu K}\alpha$ radiation (50 kV, 300 mA). TEM images were obtained on a JEOL JEM-2100F operating at 200 kV.

Preparation of [(triisopropoxysilyl)methyl]magnesium chloride

$(i\text{PrO})_3\text{SiCH}_2\text{Cl}$ (3.18 g, 12.5 mmol) was dissolved in THF (18.1 mL). Mg powder (332 mg, 13.7 mmol) was placed in a two-necked flask (50 mL) to which the THF solution of $(i\text{PrO})_3\text{SiCH}_2\text{Cl}$ (9.4 mL) was added dropwise under continuous



stirring. 3 drops of dibromoethane were then added to the mixture, and the flask was heated to 80 °C. The remaining THF solution of (iPrO)₃SiCH₂Cl was added dropwise over 10 min. The mixture was then stirred at room temperature for 4 h. The resulting solution of (iPrO)₃SiCH₂MgCl was used in the cross-coupling reaction without further purification.

Preparation of 3,8-bis[(triisopropoxysilyl)methyl]-1,10-phenanthroline (1a)

3,8-Dibromo-1,10-phenanthroline (1.49 g, 4.4 mmol) and a stirring bar were placed in an autoclave (125 mL) with a PTFE inner vessel and Ni(dppp)Cl₂ (138 mg, 6 mol%) and THF (50 mL) were gradually added. A THF solution of (iPrO)₃SiCH₂MgCl (12.5 mmol) was added dropwise over 3 min under continuous stirring. The autoclave was sealed and stirred at room temperature for 1 h, and then heated to 140 °C. After 17 h, the mixture was cooled to room temperature and then quenched with water. The mixture was extracted with CHCl₃ and the organic layer was washed with brine and dried over Na₂SO₄. The solvents were removed by rotary evaporator. The crude product was dissolved in *n*-hexane and stirred for 15 min. The mixture was filtered through a Celite pad and the solvent was removed by rotary evaporator. The crude product was purified by silica gel column chromatography (*n*-hexane/AcOEt) to give the Phen-PMO precursor, 3,8-bis[(triisopropoxysilyl)methyl]-1,10-phenanthroline (**1a**), as a pale-yellow solid (1.11 g, 41%). ¹H NMR (600 MHz, CDCl₃): δ 9.00 (d, *J* = 2.1 Hz, 2H), 8.00 (d, *J* = 2.1 Hz, 2H), 7.65 (s, 2H), 4.21 (sept, *J* = 6.1 Hz, 6H), 2.36 (s, 4H), 1.15 ppm (d, *J* = 6.1 Hz, 36H). ¹³C{¹H} NMR (151 MHz, CDCl₃): δ 151.9, 143.9, 134.8, 133.4, 127.9, 126.2, 65.7, 25.7, 19.6 ppm. ²⁹Si{¹H} NMR (119 MHz, CDCl₃): δ −56.5 ppm. Anal. calcd for C₃₂H₅₂N₂O₆Si₂: C, 62.30; H, 8.50; N, 4.54. Found: C, 62.30; H, 8.90; N, 4.50.

Preparation of Phen-PMO 3

To a screw-capped vial (110 mL) equipped with a stirring bar, P123 (0.811 g), KCl (5.17 g), distilled water (28.5 mL), and concentrated hydrochloric acid (4.05 mL) were added under ambient conditions, and the vial was sealed. The mixture was cooled to 0 °C and allowed to stand until the surfactant was completely dissolved. The mixture was then heated to 45 °C and stirred for 30 min. An ethanol solution (1.0 mL) of Phen-PMO precursor **1a** (384 mg, 0.623 mmol) and 1,2-bis(triethoxysilyl)ethane (1.25 g, 3.52 mmol) was added to the mixture at 45 °C and the resulting mixture was stirred at 45 °C for 1 day. The mixture was then heated to 100 °C and allowed to stand for 1 day. After cooling to room temperature, a pale pink precipitate was collected by filtration, washed with water, and dried under vacuum at 50 °C. The precipitate was then suspended in a solution of 2 M HCl (2.8 mL)/EtOH (100 mL) and then stirred overnight at room temperature. The precipitate was collected by filtration, washed with water and ethanol, and dried under vacuum at 50 °C to give Phen-PMO 3 (667 mg).

Immobilization of Co(OAc)₂ on Phen-PMO 3

Phen-PMO 3 (201 mg) was charged in a three-neck flask (50 mL) equipped with a mechanical stirring system. After drying Phen-

PMO 3 in vacuum at 60 °C for 2 h, dehydrated EtOH (25 mL) was added, and the solution was stirred for 1 h. A solution of Co(OAc)₂ (53 mg, 0.3 mmol) in EtOH (20 mL) was then added dropwise for 30 min with stirring. After the addition, the slurry was stirred at room temperature for 2 h and then at 60 °C for 16 h. After cooling to room temperature, the slurry was filtered through a PTFE membrane and then washed with dehydrated EtOH. The obtained solid was finally dried under vacuum to give Co(OAc)₂@Phen-PMO 4 (178 mg).

Hydrosilylation of phenylacetylene

Co(OAc)₂@Phen-PMO 4 (11 mg, 2.4 μmol/Co), THF (1 mL), phenylacetylene (51 mg, 0.5 mmol), and PhSiH₃ (68 mg, 0.6 mmol) were gradually added in a screw-capped vial (10 mL). After the mixture was stirred at 100 °C for 2 h, mesitylene was added as an internal standard at room temperature. The product yield was determined by ¹H NMR analysis.

Conclusions

This study reported the synthesis of Phen-PMO 3, in which the Phen moieties were bridged to the organosilica framework through a methylene linker, through the co-condensation of 3,8-bis[(triisopropoxysilyl)methyl]-1,10-phenanthroline (**1a**) and 1,2-bis(triethoxysilyl)ethane in the presence of P123 as the template surfactant under acidic conditions. Phen-PMO 3 had an ordered 2-D hexagonal mesoporous structure as confirmed by the nitrogen adsorption/desorption analysis, XRD, and TEM results. Co(OAc)₂ was immobilized on Phen-PMO 3 to afford an immobilized complex, Co(OAc)₂@Phen-PMO 4, which exhibited good catalytic activity for the alkyne hydrosilylation reaction. The application of Phen-PMO 3 as a solid ligand for other metal complexes is under investigation. The results of this study reveal the great potential of Phen-PMO 3 in catalysis.

Author contributions

Xiao-Tao Lin, Yusuke Ishizaka, and Yoshifumi Maegawa investigated the work. Katsuhiko Takeuchi verified the methodology. Shinji Inagaki supervised this work and helped in writing, reviewing, and editing of the manuscript. Kazuhiro Matsumoto verified the methodology, supervised the work, and wrote the original draft. Jun-Chul Choi devised the conceptual ideas and helped in the supervision, writing, reviewing, and editing of the manuscript.

Conflicts of interest

There are no conflicts to declare.

Acknowledgements

We thank the New Energy and Industrial Technology Development Organization (NEDO) for partially supporting this research (project code: P19004).



Notes and references

- 1 S. Inagaki, S. Guan, Y. Fukushima, T. Ohsuna and O. Terasaki, *J. Am. Chem. Soc.*, 1999, **121**, 9611.
- 2 T. Asefa, M. J. MacLachlan, N. Coombs and G. A. Ozin, *Nature*, 1999, **402**, 867.
- 3 B. J. Melde, B. T. Holland, C. F. Blanford and A. Stein, *Chem. Mater.*, 1999, **11**, 3302.
- 4 (a) W. Wang, J. E. Lofgreen and G. A. Ozin, *Small*, 2010, **6**, 2634; (b) N. Mizoshita, T. Tani and S. Inagaki, *Chem. Soc. Rev.*, 2011, **40**, 789; (c) P. Van Der Voort, D. Esquivel, E. De Canck, F. Goethals, I. Van Driessche and F. J. Romero-Salguero, *Chem. Soc. Rev.*, 2013, **42**, 3913; (d) J. G. Croissant, X. Cattoën, M. Wong Chi Man, J.-O. Durand and N. M. Khashab, *Nanoscale*, 2015, **7**, 20318; (e) B. Karimi, N. Ganji, O. Pourshiani and W. R. Thiel, *Prog. Mater. Sci.*, 2022, **125**, 100896.
- 5 (a) U. Díaz, D. Brunel and A. Corma, *Chem. Soc. Rev.*, 2013, **42**, 4083; (b) Y. Liang, *Nanoscale Adv.*, 2021, **3**, 6827.
- 6 For selected examples, see: (a) C. Baleizão, B. Gigante, D. Das, M. Álvaro, H. Garcia and A. Corma, *J. Catal.*, 2004, **223**, 106; (b) P. Borah, X. Ma, K. T. Nguyen and Y. Zhao, *Angew. Chem., Int. Ed.*, 2012, **51**, 7756; (c) D. Zhang, J. Xu, Q. Zhao, T. Cheng and G. Liu, *ChemCatChem*, 2014, **6**, 2998; (d) H. Takeda, M. Ohashi, Y. Goto, T. Ohsuna, T. Tani and S. Inagaki, *Adv. Funct. Mater.*, 2016, **26**, 5068.
- 7 M. Waki, Y. Maegawa, K. Hara, Y. Goto, S. Shirai, Y. Yamada, N. Mizoshita, T. Tani, W. Chun, S. Muratsugu, M. Tada, A. Fukuoka and S. Inagaki, *J. Am. Chem. Soc.*, 2014, **136**, 4003.
- 8 For selected examples, see: (a) R. Jin, K. Liu, D. Xia, Q. Qian, G. Liu and H. Li, *Adv. Synth. Catal.*, 2012, **354**, 3265; (b) A. N. Prasad, B. M. Reddy, E.-Y. Jeong and S.-E. Park, *RSC Adv.*, 2014, **4**, 29772; (c) F. Zhou, X. Hu, M. Gao, T. Cheng and G. Liu, *Green Chem.*, 2016, **18**, 5651; (d) E. Gu, W. Zhong and X. Liua, *RSC Adv.*, 2016, **6**, 98406.
- 9 For selected examples, see: (a) S. p. Shylesh, M. Jia, A. Seifert, S. Adappa, S. Ernsta and W. R. Thiel, *New J. Chem.*, 2009, **33**, 717; (b) X. Shi, B. Fan, H. Li, R. Li and W. Fan, *Microporous Mesoporous Mater.*, 2014, **196**, 277; (c) D. Elhamifar and E. Nazari, *ChemPlusChem*, 2015, **80**, 820; (d) A. Lazar, S. Silpa, C. P. Vinod and A. P. Singh, *Mol. Catal.*, 2017, **440**, 66.
- 10 For recent examples, see: (a) M. Waki, S. Shirai, K.-i. Yamanaka, Y. Maegawa and S. Inagaki, *RSC Adv.*, 2020, **10**, 13960; (b) S. Kataoka and S. Inagaki, *Eur. J. Inorg. Chem.*, 2020, **43**, 4083; (c) A. M. Kaczmarek, Y. Maegawa, A. Abalymov, A. G. Skirtach, S. Inagaki and P. Van Der Voort, *ACS Appl. Mater. Interfaces*, 2020, **12**, 13540.
- 11 For selected examples, see: (a) A. Jana, J. Mondal, P. Borah, S. Mondal, A. Bhaumik and Y. Zhao, *Chem. Commun.*, 2015, **51**, 10746; (b) H. Duan, M. Li, G. Zhang, J. R. Gallagher, Z. Huang, Y. Sun, Z. Luo, H. Chen, J. T. Miller, R. Zou, A. Lei and Y. Zhao, *ACS Catal.*, 2015, **5**, 3752; (c) S. Zhang, H. Wang, M. Li, J. Han, X. Liu and J. Gong, *Chem. Sci.*, 2017, **8**, 4489; (d) S. Ishikawa, Y. Maegawa, M. Waki and S. Inagaki, *ACS Catal.*, 2018, **8**, 4160; (e) Y. Naganawa, Y. Maegawa, H. Guo, S. S. Gholap, S. Tanaka, K. Sato, S. Inagaki and Y. Nakajima, *Dalton Trans.*, 2019, **48**, 5534; (f) X.-T. Lin, K. Matsumoto, Y. Maegawa, K. Takeuchi, N. Fukaya, K. Sato, S. Inagaki and J.-C. Choi, *New J. Chem.*, 2021, **45**, 9501; (g) S. Zhang, M. Li, W. Qiu, J. Han, H. Wang and X. Liu, *Appl. Catal., B*, 2019, **259**, 118113; (h) M. Shimizu, K. Michikawa, Y. Maegawa, S. Inagaki and K.-i. Fujita, *ACS Appl. Nano Mater.*, 2020, **3**, 2527.
- 12 For selected reviews, see: (a) P. G. Sammes and G. Yahiolu, *Chem. Soc. Rev.*, 1994, **23**, 327; (b) G. Accorsi, A. Listorti, K. Yoosafa and N. Armaroli, *Chem. Soc. Rev.*, 2009, **38**, 1690; (c) A. Bencini and V. Lippolis, *Coord. Chem. Rev.*, 2010, **254**, 2096.
- 13 For selected examples, see: (a) K. Gao and N. Yoshikai, *Angew. Chem., Int. Ed.*, 2011, **50**, 6888; (b) B. L. Tran, B. Li, M. Driess and J. F. Hartwig, *J. Am. Chem. Soc.*, 2014, **136**, 2555; (c) F. Teng, J. Cheng and C. Bolm, *Org. Lett.*, 2015, **17**, 3166; (d) S. Nakatani, Y. Ito, S. Sakurai, T. Kodama and M. Tobisu, *J. Org. Chem.*, 2020, **85**, 7588.
- 14 For selected examples of Phen-containing PMO, see: (a) X. Guo, X. Wang, H. Zhang, L. Fu, H. Guo, J. Yu, L. D. Carlos and K. Yang, *Microporous Mesoporous Mater.*, 2008, **116**, 28; (b) X. Guo, H. Guo, L. Fu, R. Deng, W. Chen, J. Feng, S. Dang and H. Zhang, *J. Phys. Chem. C*, 2009, **113**, 2603; (c) B. Yan and Y.-J. Gu, *Inorg. Chem. Commun.*, 2013, **34**, 75; (d) B. Xiao, J. Zhao, X. Liu, P. Wang and Q. Yang, *Microporous Mesoporous Mater.*, 2014, **199**, 1.
- 15 (a) C. Eaborn, *Pure Appl. Chem.*, 1969, **19**, 375; (b) W. Yao, R. Li, H. Jiang and D. Han, *J. Org. Chem.*, 2018, **83**, 2250; (c) H. Matsukawa, M. Yoshida, T. Tsunenari, S. Nozawa, A. Sato-Tomita, Y. Maegawa, S. Inagaki, A. Kobayashi and M. Kato, *Sci. Rep.*, 2019, **9**, 15151; (d) S. Shirai and S. Inagaki, *New J. Chem.*, 2021, **45**, 6120.
- 16 D. J. Brondani, R. J. P. Corriu, S. El Ayoubi, J. J. E. Moreau and M. Wong Chi Man, *J. Organomet. Chem.*, 1993, **451**, C1.
- 17 M. Waki and S. Inagaki, *Inorg. Chem. Front.*, 2022, **9**, 3669.
- 18 For selected reviews, see: (a) J.-W. Park, *Chem. Commun.*, 2022, **58**, 491; (b) L. D. de Almeida, H. Wang, K. Junge, X. Cui and M. Beller, *Angew. Chem., Int. Ed.*, 2021, **60**, 550; (c) J. Sun and L. Deng, *ACS Catal.*, 2016, **6**, 290.
- 19 For selected examples of α -selective Co-catalysed hydrosilylation, see: (a) J. Guo and Z. Lu, *Angew. Chem., Int. Ed.*, 2016, **55**, 10835; (b) Z. Zuo, J. Yang and Z. Huang, *Angew. Chem., Int. Ed.*, 2016, **55**, 10839.
- 20 For selected examples of β -trans-selective Co-catalysed hydrosilylation, see: (a) C. Wu, W. J. Teo and S. Ge, *ACS Catal.*, 2018, **8**, 5896; (b) G. Wu, U. Chakraborty and A. J. von Wangelin, *Chem. Commun.*, 2018, **54**, 12322; (c) Z. Mo, J. Xiao, Y. Gao and L. Deng, *J. Am. Chem. Soc.*, 2014, **136**, 17414.
- 21 For selected examples of β -cis-selective Co-catalysed hydrosilylation, see: (a) W. J. Teo, C. Wang, Y. W. Tan and S. Ge, *Angew. Chem., Int. Ed.*, 2017, **56**, 4328; (b) X. Du, W. Hou, Y. Zhang and Z. Huang, *Org. Chem. Front.*, 2017, **4**, 1517.
- 22 Y. Saitoh, T. Koizumi, K. Osakada and T. Yamamoto, *Can. J. Chem.*, 1997, **75**, 1336.

